ATLAST ULE Mirror Segment Performance Analytical Predictions Based on Thermally Induced Distortions

Michael J. Eisenhower* [a], Lester M. Cohen[a], Lee D. Feinberg[b], Gary W. Matthews[c], Joel A. Nissen[d], Sang C. Park[a], Hume L. Peabody[b]

a. Smithsonian Astrophysical Observatory, Cambridge, MA 02140 USA
b. NASA Goddard Space Flight Center, Greenbelt MD 02771 USA
c. Harris Corporation (Former Exelis Inc.), Rochester NY 14606 USA
d. NASA Jet Propulsion Laboratory, Pasadena, CA 91011 USA

ABSTRACT

The Advanced Technology Large-Aperture Space Telescope (ATLAST) is a concept for a 9.2 m aperture space-borne observatory operating across the UV/Optical/NIR spectra. The primary mirror for ATLAST is a segmented architecture with pico-meter class wavefront stability. Due to its extraordinarily low coefficient of thermal expansion, a leading candidate for the primary mirror substrate is Corning's ULE® titania-silicate glass. The ATLAST ULE® mirror substrates will be maintained at 'room temperature' during on orbit flight operations minimizing the need for compensation of mirror deformation between the manufacturing temperature and the operational temperatures. This approach requires active thermal management to maintain operational temperature while on orbit. Furthermore, the active thermal control must be sufficiently stable to prevent time-varying thermally induced distortions in the mirror substrates. This paper describes a conceptual thermal management system for the ATLAST 9.2 m segmented mirror architecture that maintains the wavefront stability to less than 10 pico-meters/10 minutes RMS. Thermal and finite-element models, analytical techniques, accuracies involved in solving the mirror figure errors, and early findings from the thermal and thermal-distortion analyses are presented.

Keywords: ATLAST, thermal distortion, ULE, UV, HST, JWST

NOMENCLATURE

AMSD	= Advanced Mirror System Demonstrator
ATLAST	= Advanced Technology Large Aperture Space Telescope
°C	= Degree Celsius
CTE	= Coefficient of Thermal Expansion
dT	= temperature differences
e	= Emissivity
FEM	= Finite Element Model
GSFC	= Goddard Space Flight Center
HST	= Hubble Space Telescope
Hz	= Hertz
IR	= Infrared
JWST	= James Webb Space Telescope
JPL	= Jet Propulsion Laboratory
K	= Kelvin
Kg	= Kilogram
m	= Meter
mK	= Milli-Kelvin
mm	= Millimeter
m^2	= Square Meters
MSFC	= Marshall Space Flight Center
NASA	= National Aeronautics and Space Administration
NIR	= Near-infrared
pm	= pico-meter
ppb	= Parts Per Billion

PV	= Peak to Valley
RMS	= Root Mean Square
SAO	= Smithsonian Astrophysical Observatory
SFE	= Surface Figure Error
sec	= Seconds
STScI	= Space Telescope Science Institute
t	= Transmissivity
ULE®	= Ultra-Low Expansion (ULE® is a registered mark of Corning)
UV	= Ultra-Violet
uW	= Micro Watt
WFE	= Wavefront Error

1. INTRODUCTION

The Advanced Technology Large-Aperture Space Telescope (ATLAST) mission concept builds upon key technologies developed for Hubble Space Telescope (HST) and James Webb Space Telescope (JWST). ATLAST would leverage and further enhance the technological advances developed from JWST, such as deployable large segmented-mirror arrays. This mission concept is led by the NASA Goddard Space Flight Center in Greenbelt, Maryland and is currently studying the scientific and technical requirements and costs associated with building a successor to HST and JWST. The study team also includes the Space Telescope Science Institute (STScI) in Baltimore, Maryland, the Jet Propulsion Laboratory (JPL) in Pasadena, California, the Marshall Space Flight Center (MSFC) in Huntsville, Alabama, Harris Corporation (former Exelis) in Rochester, NY, and the Smithsonian Astrophysical Observatory (SAO) in Cambridge, MA.

The Advanced Technology Large-Aperture Space Telescope (ATLAST) is under a pre-proposal concept study for a 9.2 m aperture space-borne observatory operating across the UV/Optical/NIR spectra. The primary mirror for ATLAST is a segmented architecture with pico-meter class wavefront stability. Due to its extraordinarily low coefficient of thermal expansion a leading candidate for the primary mirror substrate is Corning's ULE® titania-silicate glass. The ATLAST ULE® mirror substrates will be maintained at 'room temperature' during on orbit flight operations minimizing the need for compensation of mirror deformation between the manufacturing temperature and the operational temperatures. This approach requires active thermal management to maintain operational temperature while on orbit. Furthermore, the active thermal control must be sufficiently stable to prevent time-varying thermally induced distortions in the mirror substrates. The current goal for this mirror substrate level study is to maintain the wavefront error (WFE) to less than 10 pico-meters/10 minutes (or surface figure error, SFE, of 5 pico-meters/10 minutes RMS). To achieve these ambitious goals, the observatory needs to be thermally and structurally very stable, which can be achieved by operating in the Sun-Earth L2 orbit — the same orbit and environment chosen for the James Webb Space Telescope.

Illustrated in Figure 1 below is the artist conceptual rendering of ATLAST in the on-orbit operational configuration with the sunshade and telescope elements fully deployed. [1]

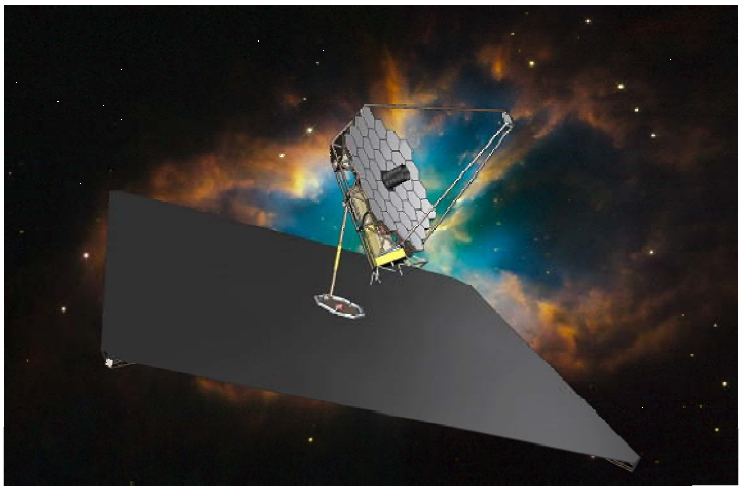

Figure 1. Artist conceptual rendering of 9.2 m Aperture ATLAST

Depicted in Figure 2 below is the conceptual design of ATLAST Telescope Element with scientific instrument payload suite in the 'stowed' configuration for launch and the 'deployed' on-orbit operational configuration. Note that the current concept of 9.2m aperture ATLAST telescope includes 36 primary mirror segments and a steerable secondary mirror: both include baffles for stray light management.

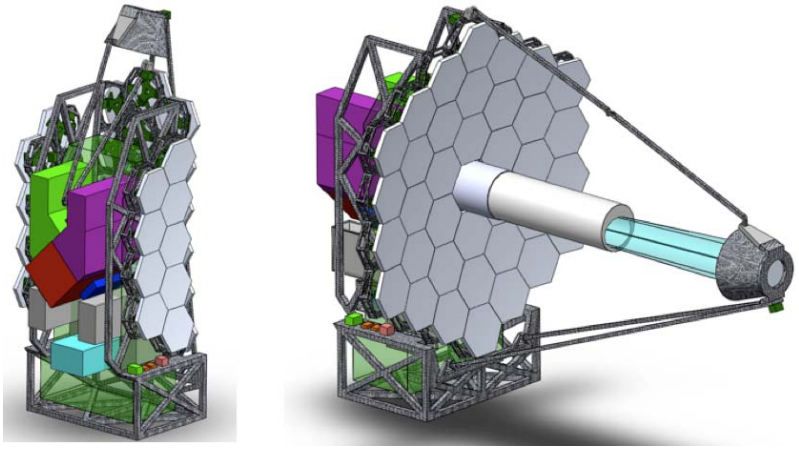

Figure 2. The conceptual design of ATLAST Telescope Element with scientific instrument payload suite in the 'stowed' configuration for launch (left view) and the 'deployed' on-orbit operational configuration (right view).

As a part of on-going conceptual studies, this study focused solely on the mirror segment level in order to characterize the local behaviors of mirror distortions induced by its thermal environment. This study was methodically performed in a sequential manner to isolate individual variables of a heater control system that may have impacts to the mirror optical surface distortions. Harris provided a structural model of a conceptual lightweight closed back ULE® mirror. The design was based on further development of their AMSD ULE® mirror design. Shown in Figure 3 is a picture of the AMSD ULE® mirror.

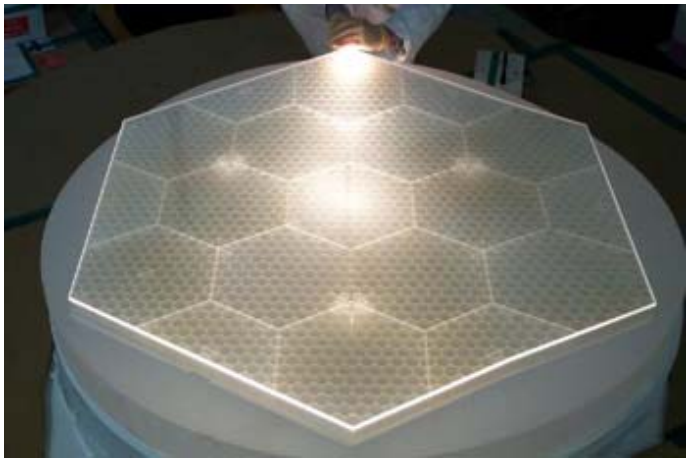

Figure 3. AMSD ULE mirror substrate similar to one used as a foundation for this thermal-distortion study.

Depicted in Table 1 is a summary of the key conceptual mirror parameters. For the purposes of this initial study we chose to focus on a bare substrate notionally held kinematically. However, the substrate has reinforcements in the core to accommodate mounting. The effects of these reinforcements are included in both the thermal and thermal distortion model results.

Table 1. ATLAST ULE Study Conceptual Mirror Segment Parameters

Parameter	**Value**
Flat to Flat Dimension	1.17 m
Point to Point Dimension	1.35 m
Radius of Curvature	16.3 m
Front Facesheet Thickness	1.7 mm
Back Facesheet Thickness	1.4 to 1.7 mm
Core Height	33 mm
Mass	11.6 kg
Areal Density	10 kg/m^2
First Frequency	180 Hz

ULE® has a very low room temperature CTE which is nominally specified as 0 +-30 ppb/K [2]. With such a low CTE variations within or between parts of the mirror becomes dominant. Different grades of ULE® have maximum allowed variations ranging from 10 to 15 ppb/K. Discussions with Corning indicate lower values are attainable by cherry picking individual parts from boules. We investigated several different CTE distributions shown in Table 2 below. Uniform: this is intended as a test case to examine response when there is no variation in the entire substrate. As delivered: this is intended as a test case where there is no variation within each facesheet but there is a variation between the front and rear facesheet. Distribution 1 and 2: Harris also provided two sets of facesheet CTE distributions for previously built ULE® mirrors of similar construction. The core was set to a constant -10 ppb/K. The distributions were based on CTE measurements of the actual facesheets and varied radially. The actual distributions are Corning Proprietary. Distribution Core: these are similar to the Distribution case but the CTE of the core was changed to +10 ppb/K

Table 2. CTE Distributions

CTE Distribution Name	Front Facesheet	Core	Rear Facesheet
Uniform	+10 ppb/K	+10 ppb/K	+10 ppb/K
As Delivered	-7 ppb/K	-10 ppb/K	-12 ppb/K
Distribution 1	Measured 1 Front	-10 ppb/K	Measured 1 Back
Distribution 2	Measured 2 Front	-10 ppb/K	Measured 2 Back
Distribution 1 Core	Measured 1 Front	+10 ppb/K	Measured 1 Back
Distribution 2 Core	Measured 2 Front	+10 ppb/K	Measured 2 Back

2. ANALYTICAL MODELS

Finite Element Model

The ANSYS™ finite element model of the ULE mirror used for this ATLAST study is depicted in Figure 4. It is a shell model with front and rear factsheets and a detailed representation of the core structure.

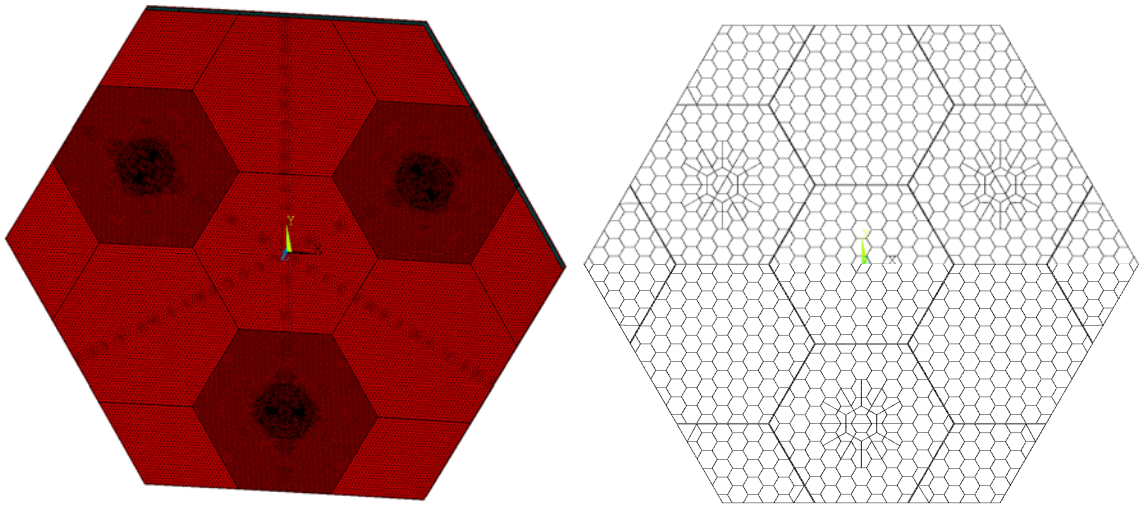

Figure 4. Mirror substrate Finite Element Model (FEM)

Thermal Model

As previously mentioned, the ATLAST ULE® mirror substrates will be maintained nominally at 'room temperature' during on orbit flight operations minimizing the need for compensation of mirror deformation between the manufacturing temperature and the operational temperatures. This approach requires active thermal management to maintain operational temperature while on orbit. A high fidelity ULE® mirror substrate thermal model was created, in Thermal Desktop™ that had coincident structural node for every thermal node. This thermal model includes the optical surface, heater plate facing rear mirror surface, mirror core, and a heater plate as depicted in Figure 5 below. The physical thermal properties of ULE® [2] were used for density, thermal conductivity, and the specific heat. The thermal optical properties included the emissivity of 0.03 for UV coating on the optical surface and the emissivity of 0.745 for the uncoated non-optical ULE® surfaces. The heater plate was represented with flat 2-D elements while the 'gap'

between the heater plate and the mirror substrate was enclosed by a notional adiabatic wall around the mirror peripheries.

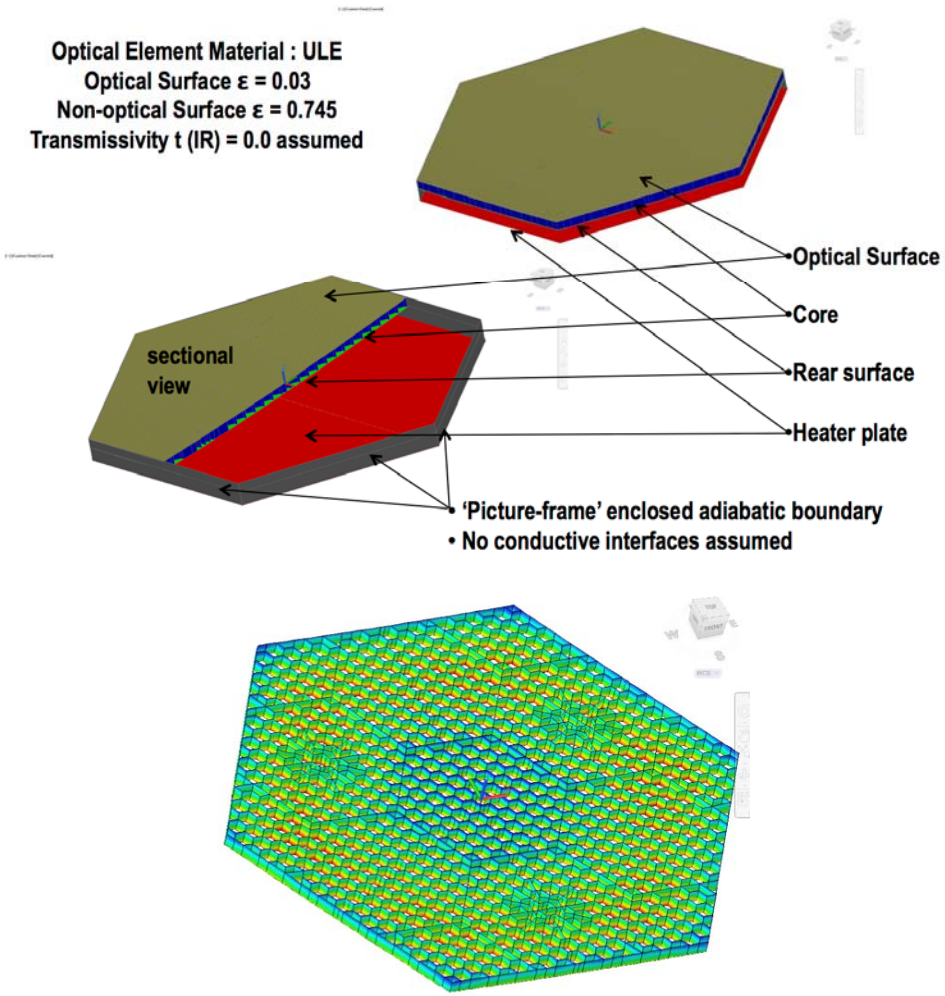

Figure 5. Mirror Substrate Thermal Model

3. CASE STUDY

There are two major categories of thermal cases considered for this study: 1.steady state, and 2.transient. The following sections of this paper will further describe each case.

SAO developed a process to export thermal results and import them into the FEM in order to calculate multiple results of the optical surface distortions in a timely manner. Calculating thermally induced mirror optical surface distortions involves first creating an analytical solution of thermal model to generate a nodal temperature map. These thermal results are then imported into the FEM of the mirror substrate in order to calculate the deformation within the mirror optical surface. The FEM results were processed through SigFit™ [Sigmadyne] to calculate the surface RMS with piston, tip, and tilt removed.

Steady State Cases

As a starting point several steady state thermal runs were performed. There were 4 steady state cases considered as follows:

Case 1. 'Baseline' 300.0000 K (26.8500 °C) heater set point where the mirror optical surface was exposed to the space environment (2.73K equivalent sink assumed).

Case 2. 300.0010 K (26.8510 °C) heater set point where the mirror optical surface was exposed to the space environment (2.73 K equivalent sink assumed).

Case 3. 300.0013 K (26.8513 °C) heater set point where the mirror optical surface was exposed to the space environment (2.73 K equivalent sink assumed).

Case 4. 300.0000 K (26.8500 °C) heater set point where the mirror optical surface was exposed to the space environment (2.73 K equivalent sink assumed) and with various heat loads, assumed as a reflected load from the secondary mirror, were imposed on the mirror optical surfaces.

The detailed description of each case follows:

Steady State Case 1: The first, baseline case, was a heater plate held uniform at 300.0000K (26.8500°C). This case established the notionally assumed baseline steady state gradient through the mirror. It also established the heater power required to maintain the mirror temperature. Currently, the baseline 300.0000 K (26.8500 °C) heater set point was chosen arbitrarily but it will be refined as this study matures and the power availabilities are better defined from the evolving separate spacecraft design efforts.

Depicted in Figure 6, below, is the energy balance of the mirror assembly with the heater plate. Note that, as previously mentioned, the heater plate was used in order to maintain the mirror temperatures nominally at 'room temperature' (293.15K or 20°C). In order to maintain the mirror assembly at that temperature, the heater plate must be maintained at nominally at 300K while dissipating 14.68 watts. As a reminder, this is based on a single segment. However, ATLAST may include as many as 36 mirror segments therefore the full compliment of mirror suite will demand for 528.6 watts, as a minimum, heater power from the spacecraft.

Also note that heater dissipation is radiated and conducted through the mirror substrate then ultimately rejected to space as depicted in Figure 6.

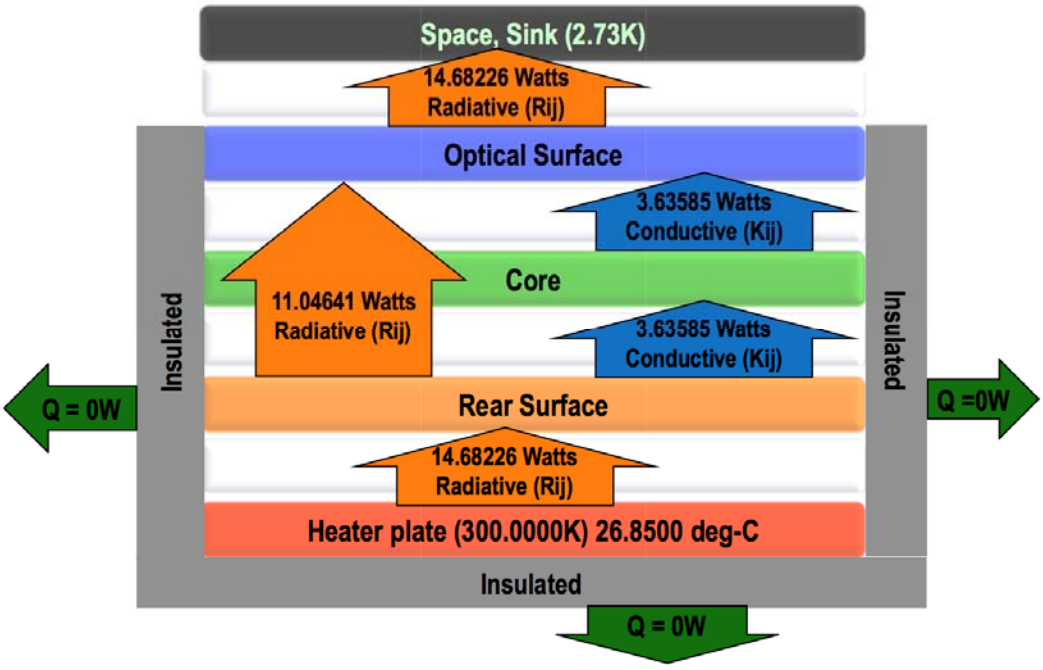

Figure 6. Mirror Assembly Energy Balance

Depicted in Figure 7, below, is an example of temperature contour resulting from the thermal model solving for steady states cases. This temperature contour was then exported to FEM for a distortion analysis. The Figure below is the results from the baseline case with a 300.0000 K heater set point, resulted in the Axial-dT of 2.05879 K, based on element surface area weighted average temperatures; ie: [(Average optical-surface) – T(Average rear-surface)]

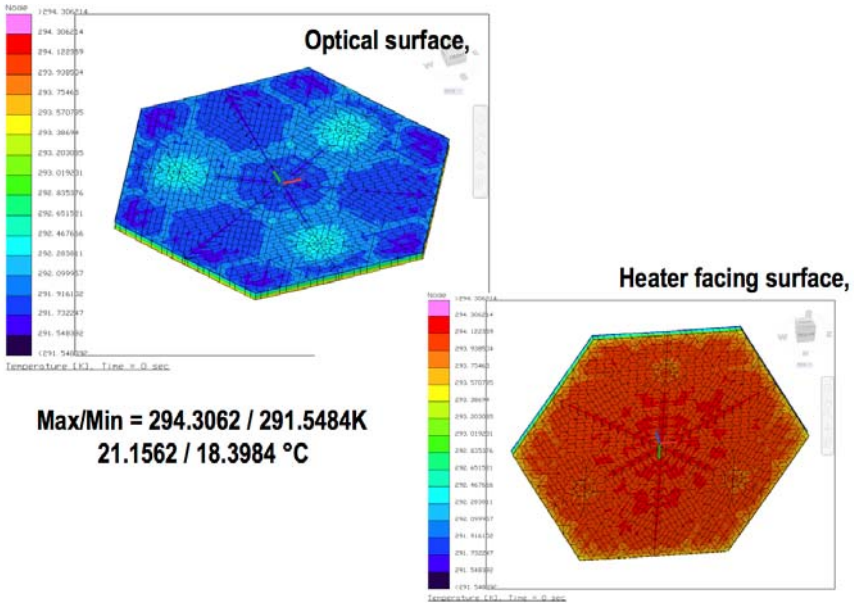

Figure 7. Temperature contour resulting from State Steady State Case Thermal Model

Steady State Cases 2 and 3: Heater Set Point Changes

Two additional steady state cases (Cases 2 and 3) where the heater set point was changed to 300.001 K and 300.0013 K were also run. These characterized the response to a 'what-if' scenario where the heater set points were changed by 1 and 1.3 mK while trying to maintain the SFE from the baseline by less than 5pico-m.

Steady State Case 2 with a 300.0010 K heater set point, or a change in 1.0 mK from the baseline, resulted in the Axial-dT of 2.05977 K where T(Average optical-surface) – T(Average rear-surface) based on element surface area weighted average temperatures.

Steady State Case 3 with a 300.0013 K heater set point, or a change in 1.3 mK from the baseline, resulted in the Axial-dT of 2.06006 K where T(Average optical-surface) – T(Average rear-surface) based on element surface area weighted average temperatures.

Table 3 below summarizes the optical results for the heater set point changes. The steady state response to a 1mK heater set point change is very dependent on the CTE distribution within the mirror. Distribution 2, which is based on actual measured properties of a similar mirror, gives surface errors that are an order of magnitude below our 5 pm SFE goal. Other distributions are near or exceed the 5 pm SFE goal. The surface stability goals are over 10 minutes so this leads us to look at transient, not just steady state response.

Table 3. Steady State Response to Heater Set Point Change

	SURFACE FIGURE ERROR RMS					
CTE	Uniform	As Delivered	Distribution 1	Distribution 2	Distribution 1 Core	Distribution 2 Core
Set Point	RMS (pm)	RMS (pm)	RMS (pm)	RMS (pm)	RMS (pm)	RMS (pm)
+1.0 mK	0.174	8.252	3.800	0.514	3.931	0.645
+1.3 mK	0.224	10.727	4.940	0.670	5.110	0.840

Steady State Case 4: Heat Load on Optical Surface

One of the driving cases for thermal loads for ATLAST would be a change in heat load on the optical surface of a mirror segment. During a slew of the telescope, the heat reflected off the secondary mirror support structure could change. In order to understand this effect steady state runs were performed with a constant heater set point (300.0000 K / 26.8500 °C) and different heat loads on the optical surface. Four individual cases were considered where the heat load on the optical surface ranged from 50 uW to 5000 uW. The results of the optical surface distortion from the external heat load are listed in the Table 4 below:

Table 4. Steady state response to optical surface heat flux while the heater plate is kept constant at 300.0000 K (or 26.8500 °C)

	SURFACE FIGURE ERROR RMS					
	Uniform	As Delivered	Distribution 1	Distribution 2	Distribution 1 Core	Distribution 2 Core
Heat Load (uW)	RMS (pm)	RMS (pm)	RMS (pm)	RMS (pm)	RMS (pm)	RMS (pm)
50	0.122	0.071	0.043	0.068	0.033	0.078
500	1.214	0.685	0.401	0.692	0.312	0.781
1000	2.411	1.383	0.811	1.372	0.633	1.550
5000	12.056	6.901	4.037	6.885	3.150	7.769

A separate and preliminary systems level thermal analysis concluded that a potential for reflected heat load from the secondary mirror as a result of slew maneuvers could be approximately 50 uW. The predicted optical distortions for all of the CTE distributions analyzed, due to the 50 uW heat load, resulted well below the 5 pm SFE goal.

Transient Cases:

Transient Case 5. Heater Set Point Changes

The previous cases were based on steady state thermal solutions. The driving requirements for ATLAST thermal stability are based on a 10 minute observation. In order to understand how the thermal mass of the ULE® substrate affects the optical response a transient analysis was performed to a 1 mK step change in heater plate temperature. Table 5 and Figure 8 show the surface RMS response as a function of time. For the As-delivered, Distribution 1, and Distribution 1 Core cases the steady state result was conservative and envelopes the transient response. For the uniform, Distribution 2, and Distribution 2 Core cases the steady state response result was not conservative and did not bound the transient result. For all CTE distributions over the 10 minute (600 sec) the surface error ranged from 1.52 to 3.67 pm RMS.

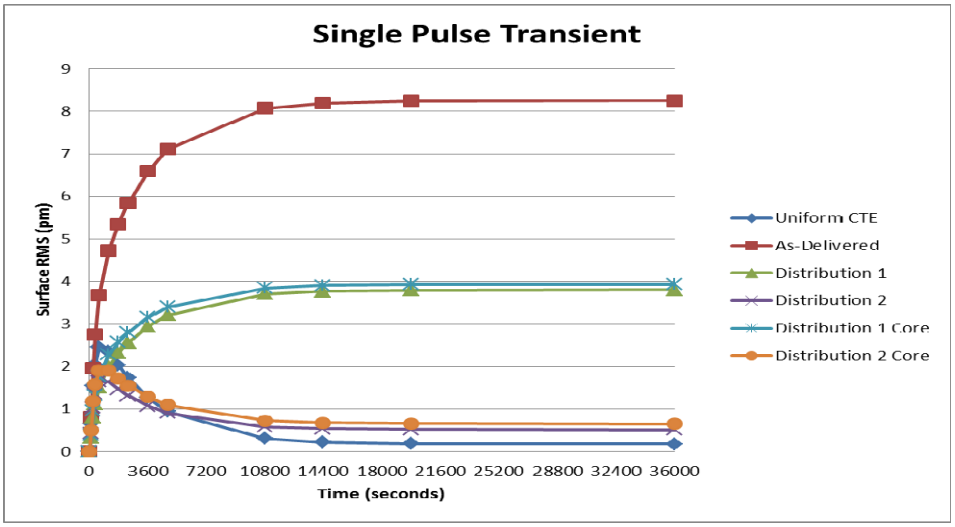

Figure 8: Transient Response to heater set point

Table 5. Transient Response to Heater Set Point Change

	SURFACE FIGURE ERROR RMS					
CTE	Uniform	As Delivered	Distribution 1	Distribution 2	Distribution 1 Core	Distribution 2 Core
Time (sec)	RMS (pm)	RMS (pm)	RMS (pm)	RMS (pm)	RMS (pm)	RMS (pm)
0	0	0	0	0	0	0
120	0.66	0.80	0.32	0.43	0.39	0.50
240	1.54	1.96	0.80	1.02	0.95	1.18
360	2.05	2.74	1.12	1.36	1.33	1.57
600	2.46	3.67	1.52	1.65	1.78	1.91
1200	2.36	4.72	2.01	1.64	2.28	1.91
1800	2.03	5.35	2.32	1.47	2.57	1.72
2400	1.73	5.85	2.57	1.31	2.81	1.55
3600	1.27	6.60	2.95	1.07	3.16	1.28
4800	0.94	7.11	3.21	0.90	3.40	1.09
10800	0.30	8.07	3.70	0.58	3.85	0.72
14400	0.22	8.19	3.77	0.54	3.90	0.67
19800	0.18	8.24	3.79	0.52	3.93	0.65
36000	0.17	8.25	3.80	0.51	3.93	0.65

The 1 mK heater set point transient case gives us an opportunity to better understand how CTE influences the distortion subject to a realistic thermal scenario. Two simple CTE variations were studied that give us further insight. The first was the effect of uniform bulk CTE, the second was the effect of front to back CTE variation.

Uniform CTE of varying magnitude

ULE® CTE is very low with average value as 0 +- 30 ppb/K. The same transient temperatures were applied to the model with entire substrate at uniform CTE's varying from -15 ppb/K to +15 ppb/K. The surface RMS responses as a function of time are shown in Figure 9.

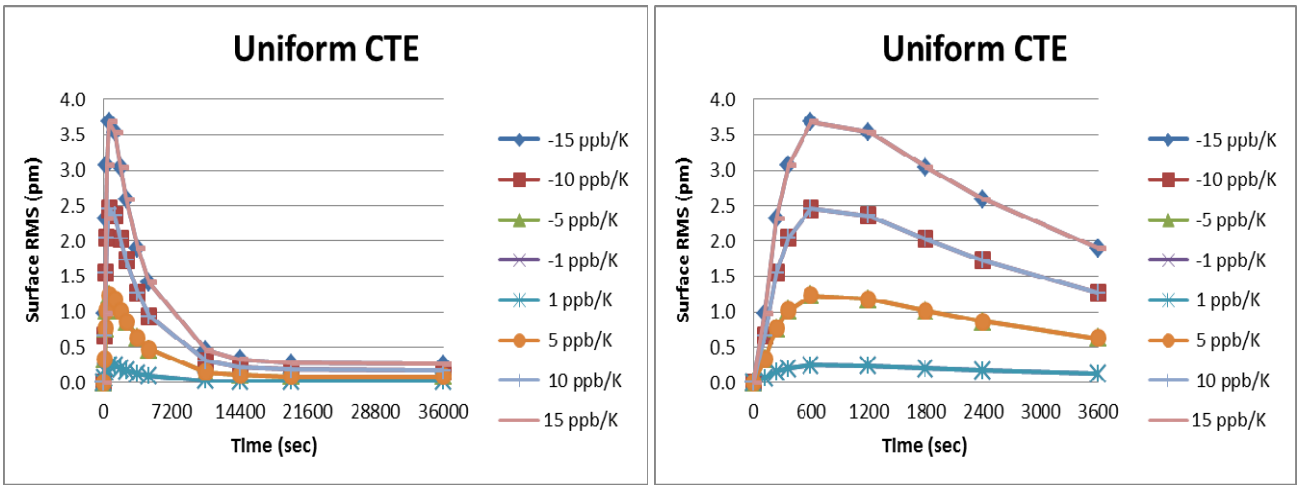

Figure 9: Transient response to a 1mK change in heater set for various uniform CTE

For all uniform CTE values we got very low surface RMS steady state responses with all less than 0.26 pm for this 1mK heater case. However, if we look at the peak transient response we see much larger response that is proportional to the uniform CTE. In Figure 10 we show the peak and steady state surface RMS response as a function of bulk CTE. For this 1 mK heater set point case we calculated the sensitivity for the SS case as 0.018 pm/(ppb/K) and the peak case as 0.246 pm/(ppb/K). Based on this, we conclude that for SS conditions any reasonable ULE uniform bulk CTE is acceptable. However for the transient case we either need a low bulk CTE, delay observations until transients have decayed, or have a fine heater control that is much better than 1 mK pulse.

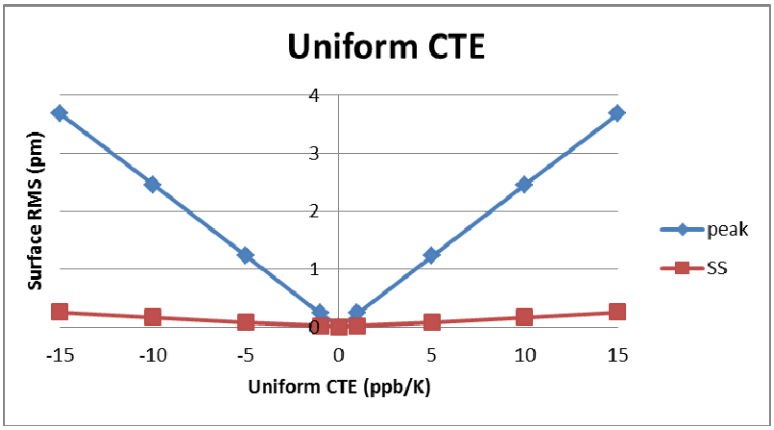

Figure 10: Peak and Steady State response to a 1 mK change in heater set for various uniform CTE

Front to Back Facesheet CTE variation

Different grades of ULE have specs on CTE variation within a boule bounded to 10 to 15 ppb/K depending on grade. A front to back CTE difference has the largest potential to distort the mirror. The same 1 mK heater transient case was applied to models with varying front to back facesheet CTE. The cases are designated FF-CTE_Core-CTE_RF-CTE, where the numbers are CTE in ppb/K (See Table 6). The surface RMS responses are shown in Figure 11.

Table 6: Front to back CTE variations analyzed

	CTE (ppb/K)			
Case	Front Facesheet	Core	Back Facesheet	Front - Back
10_10_10	10	10	10	0
11_10_9	11	10	9	2
12_10_8	12	10	8	4
13_10_7	13	10	7	6
14_10_6	14	10	6	8
15_10_5	15	10	5	10

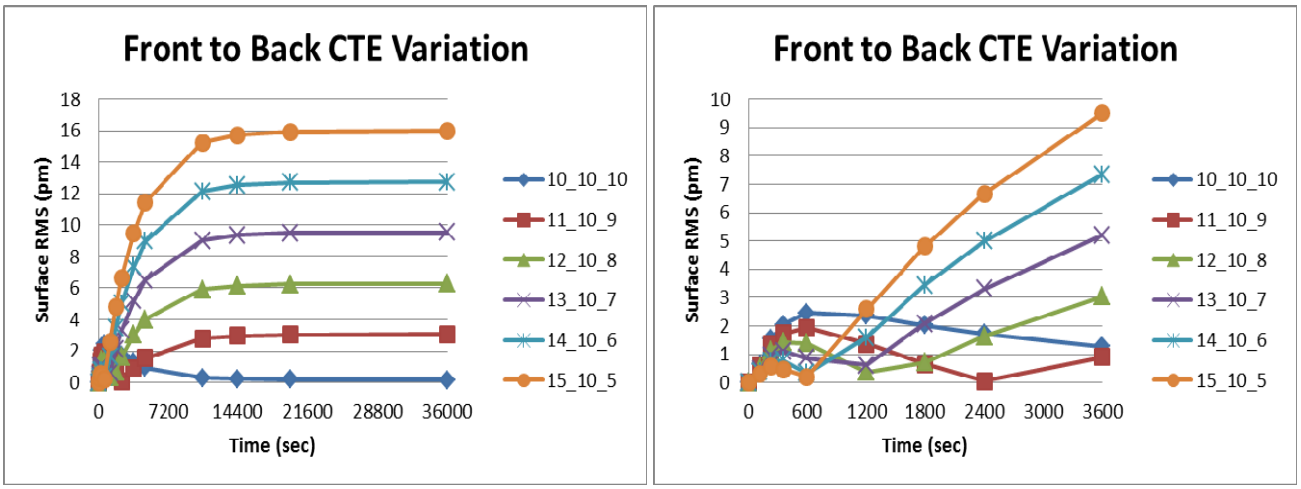

Figure 11: Transient response to a 1 mK change in heater set for various front to rear facesheet CTE differences

For all cases where there was a difference in CTE the steady state response was conservative and bounded the transient response. However over shorter time scales the response was much less. Figure 12 below shows the surface RMS as a function of front to back facesheet CTE difference. For steady state results and the 1mK heater transient we calculated the sensitivity of 1.6 pm/(ppb/K front to back CTE variation). This can be used, along the granularity of heater control, to trade the allowed front to back CTE allowed in the mirror substrate.

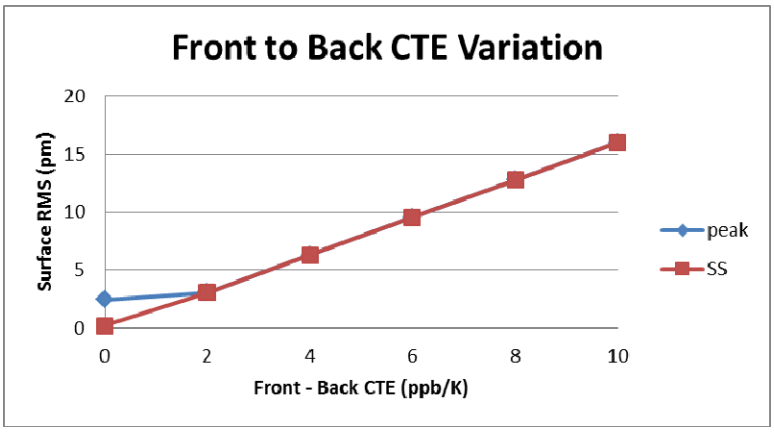

Figure 12: Peak and Steady State response to a 1 mK change in heater set for various front to back facesheet CTE differences

Transient Case 6. Heater cycling transients

In order to characterize a more realistic operational scenario, the following case was analyzed. This case includes many of the previous scenarios but is combined to simulate a possible transient behavior, where the heaters are cycling on and off, and then a notional orbital slewing of the telescope causing it to impose additional heat load on to the mirror optical surface.

For this portion of the analysis, it was assumed that the heater plate was cycling on and off at a constant period of 3 minutes that included 2x 30 seconds dwell time at each 'peak and valley' with 2x 60 seconds of ramping in between. Furthermore, the heater plate was assumed to be cycling between peaks-and valleys of 26.850 +/-0.005 °C. Note that this is just a notionally assumed operation of the heater plate in order to understand the thermal behaviors of the mirror substrate. A further detailed study is planned where realistic heater logic, once developed, will be introduced into the model to predict the thermal behavior of that system. This assumption is well within the current technologies of heater logic design. Furthermore, SAO recently demonstrated as a part of future Giant Magellan Telescope (GMT) instrument development[3], a high precision heater logic that may satisfy the required thermal stability for ATLAST.

As noted on Figure 13, after the 18000 seconds mark, it was assumed that additional heat load or 50 uW was imposed on to the mirror optical surface, simulating a reflected heat from the secondary mirror. Note that there's a small shift in temperatures at both the optical surface and the rear surface (upper plots) while the heater plate (lower plot) remained constant at their temperature peaks-and-valleys.

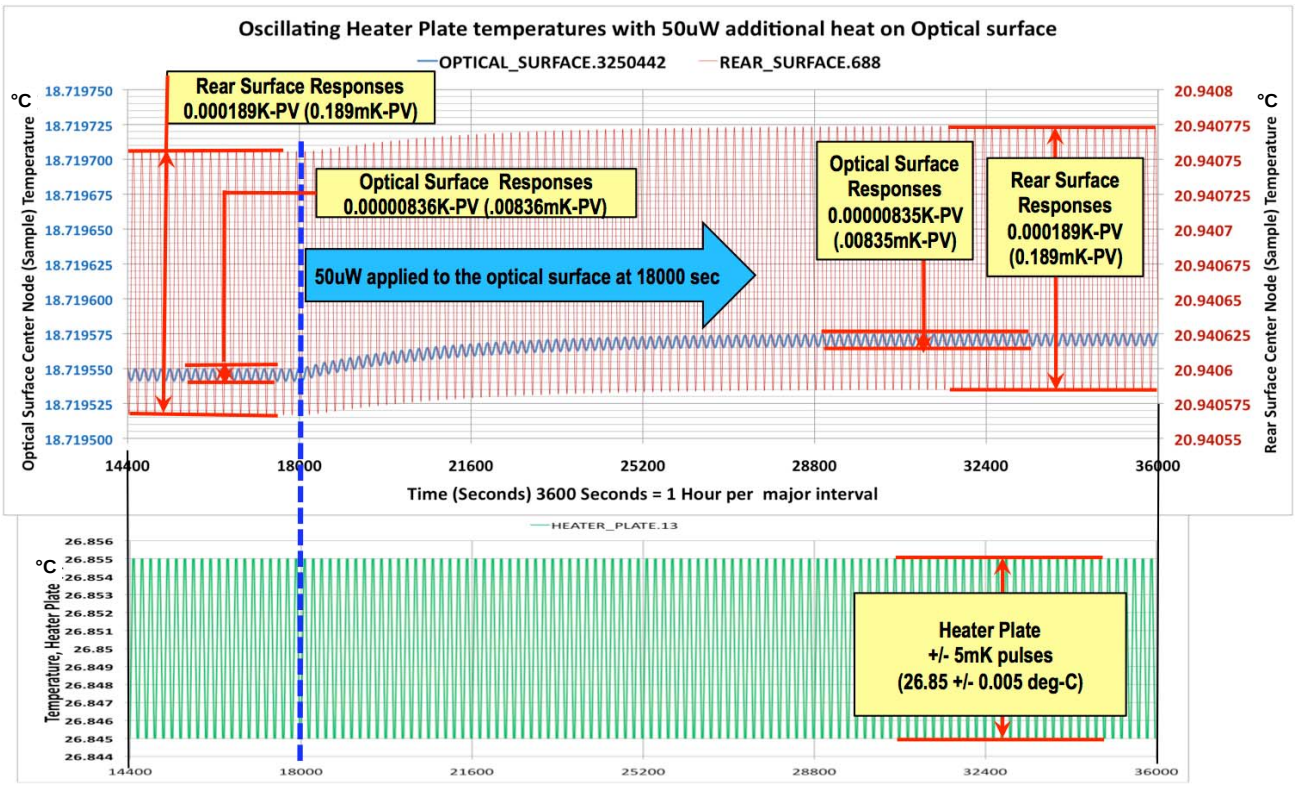

Figure 13: Heater Cycling Transient Analysis with and without the reflected heat load from the Secondary mirror.

Illustrated in the Figure 14 below, a close-up of Figure 13, are the transient behaviors of the heater plate, the mirror optical surfaces, and the mirror rear surface facing the heater plate. Between time 14400 and 18000 seconds, it was assumed that a dynamic steady state was achieved with the heater plate cycling between the set points of 26.850 +/-0.005 °C without any other external heat load. The predictions showed, while the heater plate was cycling between peaks and valleys of +/-5mK, the rear-surface facing the heater plate was only changing by +/-0.189 mK-PV, and predicted even less at the optical surface where the changes were +/-0.00836 mK-PV.

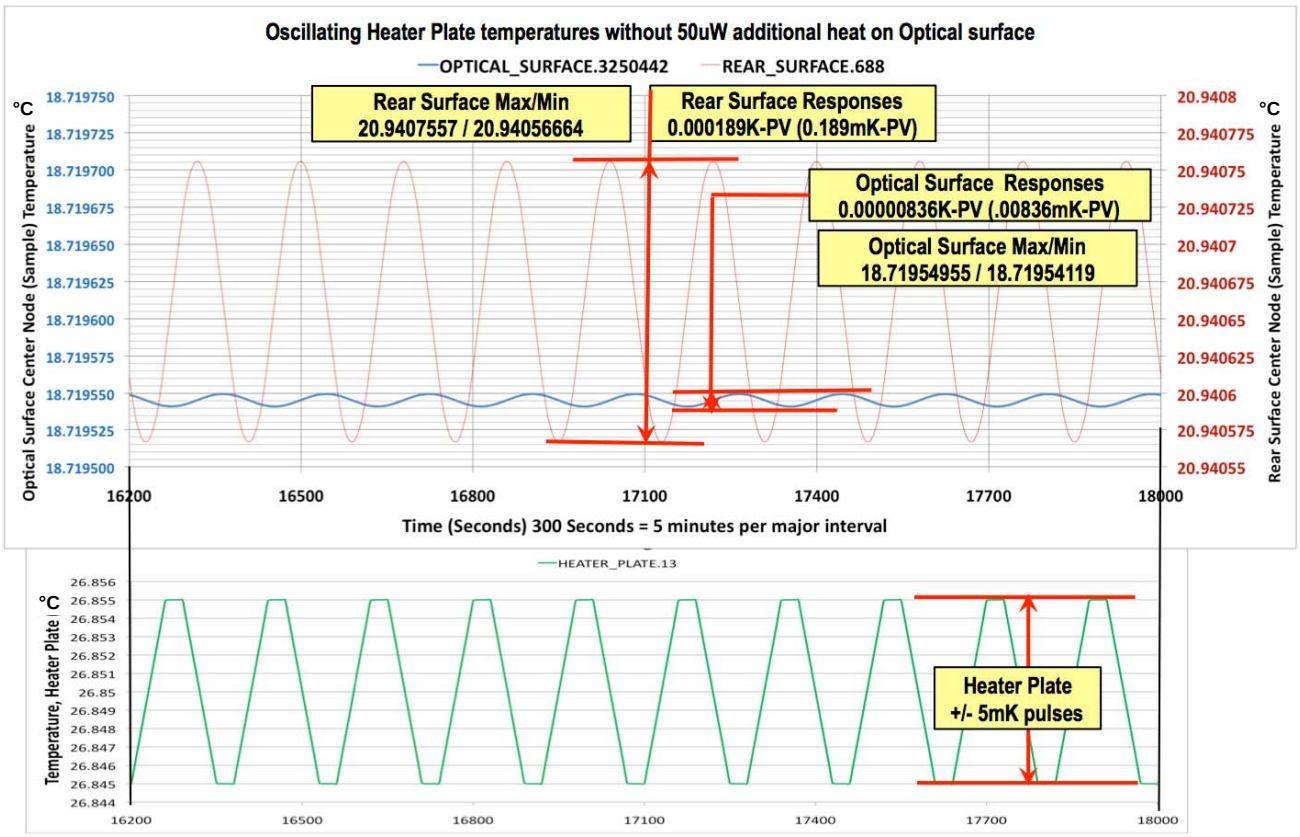

Figure 14: Heater cycling transient analysis without the reflected heat load from the Secondary mirror.

Illustrated in the Figure 15 below, a close-up of Figure 13, are the transient behaviors of the heater plate, the mirror optical surfaces, and the mirror rear surface facing the heater plate. After the time 32400seconds, it was assumed that a dynamic steady state was re-established after the 50 uW additional heat load was imposed and with the heater plate continued cycle between the set points of 26.850 +/-0.005 °C. The predictions showed, while the heater plate was cycling between peaks and valleys of +/-5 mK, the rear-surface facing the heater plate was only changing by +/-0.189mK-PV, and predicted even less at the optical surface where the changes were +/-0.00835mK-PV, virtually unnoticeable changes when compared with the dynamic steady state without the 50 uW additional heat load.

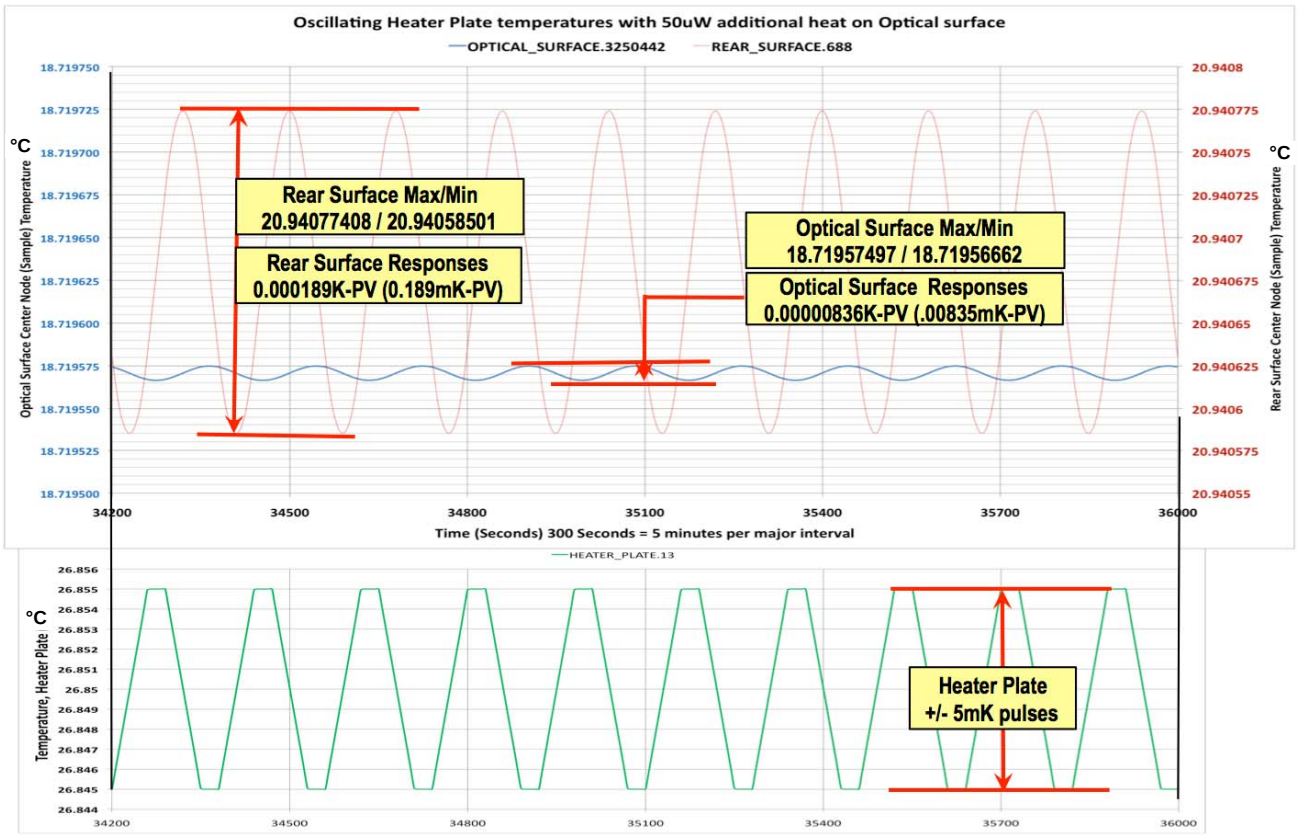

Figure 15: Heater cycling transient analysis with the 50 uW reflected heat load from the secondary mirror.

Figure 16 shows the dynamic steady state optical response just due to the heater cycling. Note that for this arbitrary heater pulse frequency and magnitude, all the CTE distributions analyzed have surface RMS vary between 1.3 and 3.1. A reduction in cycling time and or a reduction in heater plate temperature variation would reduce the response. Figure 17 shows the dynamic steady state response due to the heater cycling after the change in heat load and the system has reached a new dynamic steady state. The results are identical to precision reported by the optical results.

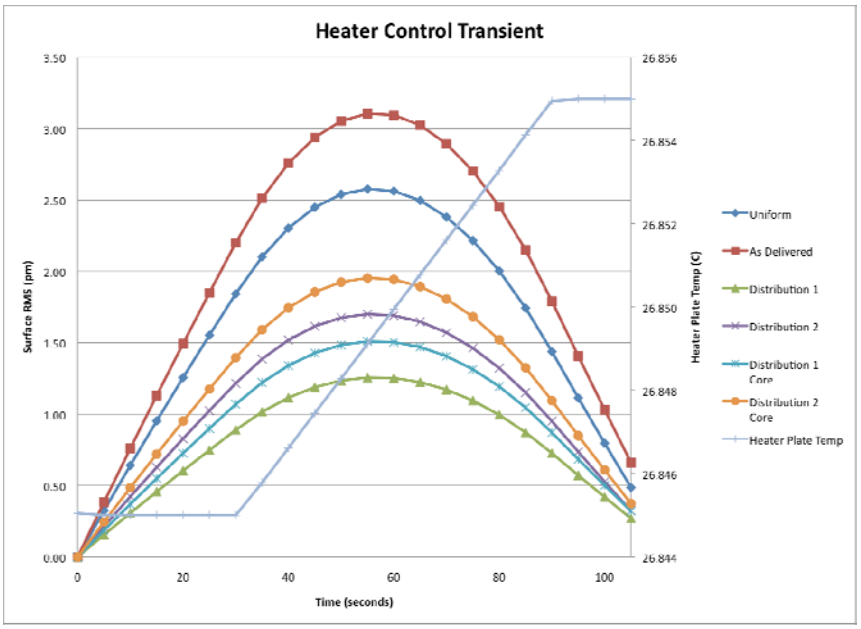

Figure 16: Transient heater cycle without imposed heat load from the SM

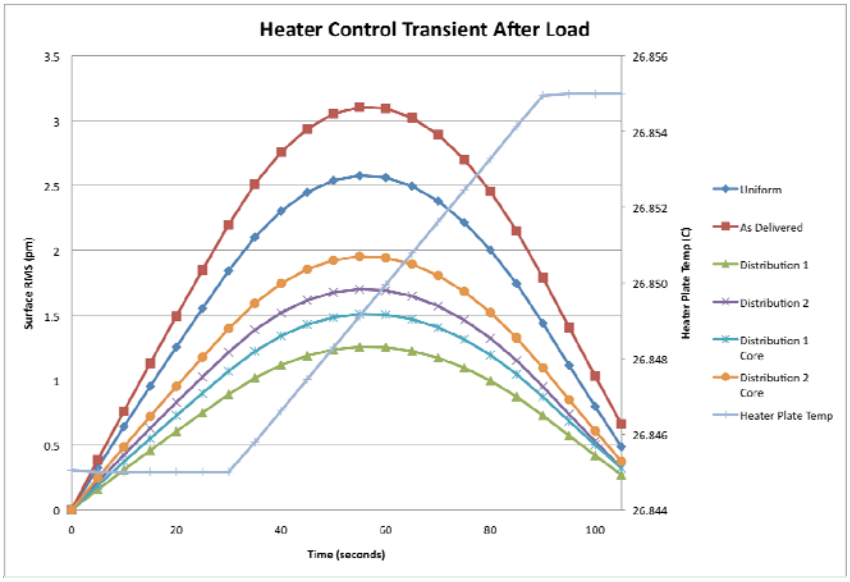

Figure 17: Transient heater cycle with the 50 uW reflected heat load from the secondary mirror.

4. CONCLUSIONS

Several steady state and transient thermal cases were run to simulate possible operational and control scenarios. The optical performance impact using several different CTE distributions within the mirror substrate were analyzed. The effects of notional heater control were analyzed and the impact on surface error was computed. The results indicated stability requirements are challenging but achievable, laying the ground work for future studies.

As stated earlier, this is a pre-proposal conceptual study where many assumptions were used to conduct this study including the heater plate performances. Due to extreme challenging thermal and structural stabilities requirements for ATLAST 9.2 m aperture telescope, a high precision heater controller will be required to maintain at the mission desirable temperatures. Furthermore, this study was performed at the mirror substrate level. Future studies will include the thermal and structural stabilities of the mirror support structures. Also, heater controllers will be developed to meet the high accuracies that would be required to meet the ATLAST expected mission performances.

REFERENCES

[1] 224th American Astronomical Society Meeting June 5th 2014 The Advanced Technology Large-Aperture Space Telescope (ATLAST) Carl Stahle, Harley Thronson et. al.

[2] CORNING ULE 7972
https://www.corning.com/media/worldwide/csm/documents/D20FD2EA-7264-43DD-B544-E1CA042B486A.pdf

[3] Proc. SPIE 9147, Ground-based and Airborne Instrumentation for Astronomy V, 91479A (6 August 2014);
The opto-mechanical design of the GMT-consortium large earth finder (G-CLEF) Author(s): Mark Mueller; Daniel Baldwin; Jacob Bean; Henry Bergner; Bruce Bigelow; Moo-Young Chun; Jeffrey Crane; Jeff Foster; Gabor Fűrész; Thomas Gauron; Dani Guzman; Edward Hertz; Andrés Jordán; Kang-Min Kim; Kenneth McCracken; Timothy Norton; Mark Ordway; Chan Park; Sang Park; William A. Podgorski; Andrew Szentgyorgyi; Alan Uomoto; In-Soo Yuk Date Published: 6 August 2014